

Differentiating Mechanistic Possibilities for the Thermal, Intramolecular [2 + 2] Cycloaddition of Allene–Ynes

Matthew R. Siebert,^{†,§} Joshua M. Osbourn,[‡] Kay M. Brummond,^{*,‡} and Dean J. Tantillo^{*,†}

Department of Chemistry, University of California - Davis, One Shields Avenue, Davis, California, 95616, and Department of Chemistry, University of Pittsburgh, Pittsburgh, Pennsylvania 15260

Received April 5, 2010; E-mail: tantillo@chem.ucdavis.edu; kbrummon@pitt.edu

Abstract: Intramolecular [2 + 2] cycloaddition reactions of allene–ynes offer a quick and efficient route to fused bicyclic ring structures. Insights into the mechanism and regiochemical preferences of this reaction are provided herein on the basis of the results of quantum chemical calculations (B3LYP/6-31+G(d,p)) and select experiments; both indicate that the reaction likely proceeds through a stepwise diradical pathway where one radical center is stabilized through allylic delocalization. The influences of the length of the tether connecting the alkyne and allene and substituent effects are also discussed.

1. Introduction and Background

Some of the earliest applications of allenes in natural product synthesis employed the [2 + 2] cycloaddition reaction.¹ A particularly powerful example involved a photoinitiated [2 + 2] cycloaddition between an allene and an enone, a method pioneered independently in the laboratories of Corey² and Eaton,³ moreover, many examples exist where these photoadducts have been creatively transformed to a variety of challenging functionalities.⁴ Considerable attention has been devoted to the study of the [2 + 2] cycloaddition reaction between *alkenes* and allenes;⁵ however, until recently, there have been only scattered reports of [2 + 2] cycloaddition reactions between *alkynes* and allenes.⁶ The first documented example of a [2 + 2] cycloaddition reaction between an allene and alkyne was reported by Applequist and Roberts in 1956.⁷ In their report, phenylacetylene and 1,2-propadiene were heated in a sealed tube to 130 °C to provide a 1% yield of 1-phenyl-3-methylenecyclobutene. Interest in the reaction has increased over the years from a mechanistic viewpoint.⁸

There has always been intrigue associated with the mechanism of [2 + 2] cycloaddition reactions because the $[\pi 2_s + \pi 2_s]$ process is forbidden based upon the orbital symmetry principles

for concerted reactions developed by Woodward and Hoffmann.⁹ However, the $[\pi 2_s + \pi 2_a]$ process is allowed with clear restrictions on the geometry of the approach for the two components, though there are a substantial number of instances where the combination of 2-ethylenic molecules lacking the special prerequisites for the $[\pi 2_s + \pi 2_a]$ process still lead to a cyclobutane. In these cases, evidence overwhelmingly favors discrete biradical or ionic intermediates.¹⁰ The literature concerning the mechanism of thermal and photoinitiated [2 + 2] cycloaddition reactions of allene–enes is vast, but very few studies exist on the mechanism of [2 + 2] cycloaddition of allene–ynes. One example was reported by Pasto where the cycloaddition of enantioenriched allenes with methyl propiolate was studied.^{8e} Two cycloadducts were formed in which 40% of the enantiomeric excess had been transferred to the products. *Ab initio* calculations indicated an anti,syn biradical intermediate is preferentially formed, and for this example, the alkyne is substituted with an ester that would provide stabilization of the inferred radical intermediate.

In 2005, one of the authors reported a thermal, intramolecular [2 + 2] cycloaddition reaction of allene–ynes to form alkylidene cyclobutenes (Figure 1).¹¹ In contrast to the studies referred to above, a few of the cycloaddition reactions studied contained

[†] University of California - Davis.

[‡] University of Pittsburgh.

[§] Current address: Department of Chemistry and Biochemistry, Texas Tech University, Lubbock, Texas 79409.

(1) Ma, S. *Chem. Rev.* **2005**, *105*, 2829–2871.

(2) Corey, E. J.; Bass, J. D.; LeMahieu, R.; Mitra, R. B. *J. Am. Chem. Soc.* **1964**, *86*, 5570–5583.

(3) Eaton, P. E. *Tetrahedron Lett.* **1964**, *5*, 3695–3698.

(4) Brummond, K. M.; Chen, H. In *Modern Allene Chemistry*; Krause, N., Hashmi, A. S. K., Eds.; Wiley: New York, 2004; Vol. 2, pp 1041–1089.

(5) Murakami, M.; Matsuda, T. In *Modern Allene Chemistry*; Krause, N., Hashmi, A. S. K., Eds.; Wiley: New York, 2004; Vol. 2, pp 727–815.

(6) Alcaide, B.; Almendros, P.; Aragoncillo, C. *Chem. Soc. Rev.* **2010**, 783–816.

(7) Applequist, D. E.; Roberts, J. D. *J. Am. Chem. Soc.* **1956**, *78*, 4012–4022.

(8) (a) Chia, H.-A.; Kirk, B. E.; Taylor, D. R. *J. Chem. Soc., Perkin Trans. 1* **1974**, 1209–1213. (b) Kirk, B. E.; Taylor, D. R. *J. Chem. Soc., Perkin Trans. 1* **1974**, 1844–1848. (c) Pasto, D. J.; Kong, W. *J. Org. Chem.* **1988**, *53*, 4807–4810. (d) Pasto, D. J.; Kong, W. *J. Org. Chem.* **1989**, *54*, 3215–3216. (e) Pasto, D. J.; Sugi, K. D.; Alonso, D. E. *J. Org. Chem.* **1992**, *57*, 1146–1150.

(9) (a) Hoffmann, R.; Woodward, R. B. *Acc. Chem. Res.* **1968**, *1*, 17–22. (b) Woodward, R. B.; Hoffmann, R. *Angew. Chem., Int. Ed. Engl.* **1969**, *8*, 781–853. (c) Woodward, R. B.; Hoffmann, R. *The Conservation of Orbital Symmetry*; Verlag Chemie 1970.

(10) (a) Siebert, M. R.; Yudin, A. K.; Tantillo, D. J. *Org. Lett.* **2007**, *10*, 57–60. (b) Nicolaou, K. C.; Lister, T.; Denton, R. M.; Gelin, C. F. *Angew. Chem., Int. Ed.* **2007**, *46*, 7501–7505. (c) Machiguchi, T.; Okamoto, J.; Takachi, J.; Hasegawa, T.; Yamabe, S.; Minato, T. *J. Am. Chem. Soc.* **2003**, *125*, 14446–14448. (d) Schuster, D. I.; Lem, G.; Kaprinidis, N. A. *Chem. Rev.* **1993**, *93*, 3–22.

(11) Brummond, K. M.; Chen, D. *Org. Lett.* **2005**, *7*, 3473–3475.

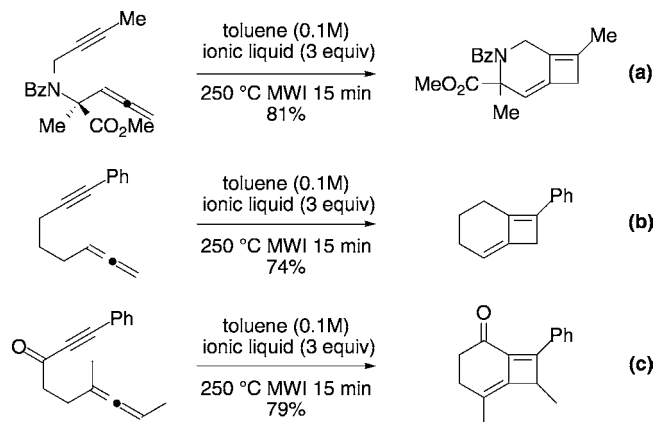
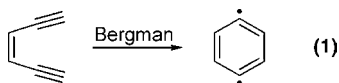


Figure 1. Representative thermal, intramolecular allene–yne [2 + 2] cycloaddition reactions. (a) Benzamide substrate containing no radical stabilizing groups. (b) Allene–yne containing a phenyl group on the alkyne as a potential radical stabilizer. (c) Allene–yne containing a carbonyl in the tether as well as a phenyl group acting as potential radical stabilizers.

no stabilizing groups appended to either the alkyne or allene, and yet good yields of the alkylidene cyclobutene were still obtained. Thus, it is less clear whether a biradical intermediate is involved.

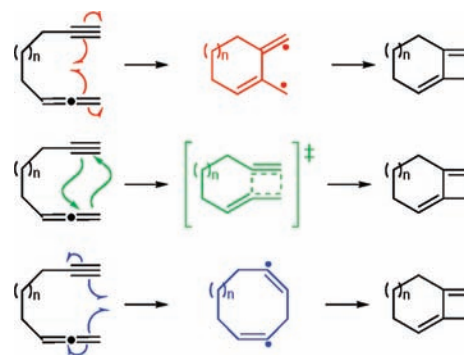
Literature examples implicating biradical intermediates in reaction mechanisms abound; however, evidence confirming their presence is much less common. Moreover, capturing and proving the existence of *thermally generated biradicals* remains the most elusive,¹² but these do make an appearance in some well-known reactions, including the Bergman reaction that involves the thermally induced cycloaromatization reaction of an ene-diyne to generate a phenylene diradical (eq 1).¹³ Relatives of the Bergman cyclization reaction include the Myers–Saito¹⁴ and Schmittel¹⁵ cyclizations of enyne-allenes. Many theoretical works have been devoted to these reactions, which involve diradical intermediates, although it has been noted that theoretical description of such pathways can be somewhat troublesome in some cases due to the involvement of both ground- and excited-state structures.¹⁶



Subsequent to the initial allene–yne [2 + 2] cycloaddition report, other examples have appeared demonstrating the utility

- (12) See the following and references therein: Cremeens, M. E.; Carpenter, B. K. *Org. Lett.* **2004**, *6*, 2349–2352.
- (13) (a) Jones, R. R.; Bergman, R. G. *J. Am. Chem. Soc.* **1972**, *94*, 660–661. (b) Bergman, R. G. *Acc. Chem. Res.* **1973**, *6*, 25–31.
- (14) (a) Myers, A. G. *Tetrahedron Lett.* **1987**, *28*, 4493–4496. (b) Saito, K.; Watanabe, T.; Takahashi, K. *Chem. Lett.* **1989**, 2099–2102.
- (15) (a) Schmittel, M.; Strittmatter, M.; Kiau, S. *Tetrahedron Lett.* **1995**, *36*, 4975–4978. (b) Schmittel, M.; Strittmatter, M.; Kiau, S. *Angew. Chem., Int. Ed. Engl.* **1996**, *35*, 1843–1845.
- (16) (a) Engels, B.; Hanrath, M. *J. Am. Chem. Soc.* **1998**, *120*, 6356–6361. (b) Engels, B.; Lennartz, C.; Hanrath, M.; Schmittel, M.; Strittmatter, M. *Angew. Chem., Int. Ed.* **1998**, *37*, 1960–1963. (c) Schreiner, P. R.; Prall, M. *J. Am. Chem. Soc.* **1999**, *121*, 8615–8627. (d) Cramer, C. J.; Kormos, B. L.; Seierstad, M.; Sherer, E. C.; Winget, P. *Org. Lett.* **2001**, *3*, 1881–1884. (e) deVisser, S. P.; Filatov, M.; Shaik, S. *Phys. Chem. Chem. Phys.* **2001**, *3*, 1242–1245. (f) Musch, P. W.; Engels, B. *J. Am. Chem. Soc.* **2001**, *123*, 5557–5562. (g) Stahl, F.; Moran, D.; von Rague Schleyer, P.; Prall, M.; Schreiner, P. R. *J. Org. Chem.* **2002**, *67*, 1453–1461. (h) Bekele, T.; Christian, C. F.; Lipton, M. A.; Singleton, D. A. *J. Am. Chem. Soc.* **2005**, *127*, 9216–9223.

Scheme 1. Potential Mechanistic Pathways in the Thermal Allene–Yne [2 + 2] Cycloaddition Reaction



of this method.¹⁷ In 2008 this methodology was utilized by Ovaska and Kyne to access the core ring structure of the sterpene class of natural products.^{17e}

Several mechanisms for these thermal allene–yne [2 + 2] cycloadditions were envisaged, including two stepwise and one concerted pathway (Scheme 1). Although orbital symmetry considerations⁹ dictate that a concerted thermal [2 + 2] reaction is allowed only if a suprafacial/antarafacial arrangement of the combining π -systems can be obtained, the perpendicular orbitals in the allene and alkyne introduce the possibility of pseudo-pericyclic, cruciaromatic, or coarctate processes.¹⁸ The two diradical mechanistic possibilities differ in the order in which the two new σ -bonds are formed and, upon *prima facie* inspection, seem as though they may be quite similar in energy.¹⁹ In addition, one may wonder the extent to which these reactions are selective for cycloaddition onto the distal, rather than the proximal, π -bond of the allene since, for the systems examined so far, it was observed that only the distal π -bond of the allene moiety reacts. Furthermore, a mechanistic understanding of this thermal allene–yne [2 + 2] cycloaddition will enable a more accurate prediction of those substrates that will successfully participate in the cycloaddition, as well as cascading diradical processes.

These issues are tackled herein using hybrid density functional theory calculations and select experiments. We first address the mechanism of the [2 + 2] cycloaddition in the absence of any substituents that could modulate the electronics of the π -systems that are involved. Second, we quantify the effect of the length of the tether connecting the alkyne and allene ($n = 0–3$, Scheme 1) on the barrier for cycloaddition, where predictions on the limits of selectivity for the terminal C=C unit will also be made. Next, the influence of carbonyl and phenyl substituents (pre-

- (17) (a) Oh, C. H.; Gupta, A. K.; Park, D. I.; Kim, N. *Chem. Commun.* **2005**, 5670–5672. (b) Jiang, X.; Ma, S. *Tetrahedron* **2007**, *63*, 7589–7595. (c) Mukai, C.; Hara, Y.; Miyashita, Y.; Inagaki, F. *J. Org. Chem.* **2007**, *72*, 4454–4461. (d) Ohno, H.; Mizutani, T.; Kadoh, Y.; Aso, A.; Miyamura, K.; Fujii, N.; Tanaka, T. *J. Org. Chem.* **2007**, *72*, 4378–4389. (e) Ovaska, T. V.; Kyne, R. E. *Tetrahedron Lett.* **2008**, *49*, 376–378. (f) Zriba, R.; Gandon, V.; Aubert, C.; Fensterbank, L.; Malacria, M. *Chem.–Eur. J.* **2008**, *14*, 1482–1491.
- (18) (a) Ross, J. A.; Seiders, R. P.; Lemal, D. M. *J. Am. Chem. Soc.* **1976**, *98*, 4325–4327. (b) Dewar, M. J. S.; Healy, E. F.; Ruiz, J. *Pure Appl. Chem.* **1986**, *58*, 67–74. (c) Herges, R. *Angew. Chem., Int. Ed. Engl.* **1994**, *33*, 255–276. (d) Herges, R. *J. Chem. Inf. Comput. Sci.* **1994**, *34*, 91–102. (e) Birney, D. M. *J. Am. Chem. Soc.* **2000**, *122*, 10917–10925.
- (19) In principle two zwitterionic pathways would also be accessible, although no such intermediates were located in the work herein. All computations were carried out in an unrestricted manner, which does not bias the results towards radical pathways; see Computational Methods for further discussion.

serving a terminal allene) on the mechanism is delineated. Lastly, calculations and experiments on cyclopropane substituted allene–ynes are described that provide evidence for the presence of a diradical intermediate.

Computational Methods

All structures were fully optimized in the gas-phase²⁰ using GAUSSIAN03²¹ without symmetry constraints at the uB3LYP²²/6-31+G(d,p) level of theory with spin symmetry broken (by invoking the guess=(mix,always) designation). Three sets of energies are reported herein: zero-point energy corrected (unscaled) electronic energies computed with the B3LYP/6-31+G(d,p) and mPW1PW91/6-31+G(d,p)//B3LYP/6-31+G(d,p)²³ methods and Gibbs free energies computed with the B3LYP/6-31+G(d,p) method at 250 °C (which includes zero-point energy correction). Each structure was classified as a minimum or transition-state structure by frequency analysis. Intrinsic reaction coordinate calculations were used to help locate minima associated with many transition-state structures described herein.²⁴ Structural drawings were produced using *Ball&Stick*.²⁵

The unrestricted nature of the uB3LYP (guess=(mix,always)) calculations allows for determination of the lowest-energy (gas-phase) singlet state—be it zwitterionic or diradical; the program is not biased in one direction and will converge on the lowest-energy solution (although the gas-phase approximation may disfavor zwitterions).²⁰ The uB3LYP method (usually with basis sets similar to but smaller than 6-31+G(d,p)) has been used in many studies to describe the reactivity of singlet diradicals²⁶ and to compute singlet/triplet energy gaps.²⁷ Comparisons between results obtained with uB3LYP and CISD,^{26a} CASSCF,^{26c,e} and full CI^{26b} calculations indicate that relative energies computed with the uB3LYP method generally differ by less than 5 kcal/mol from those obtained with

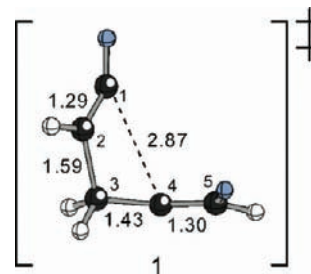


Figure 2. Transition-state structure for the thermally allowed⁹ supra/antafacial [2 + 2] cycloaddition of allene and ethyne. Select distances are displayed in angstroms (Å). Blue atoms show the positions connected in the intramolecular variation described below.

the more computationally intensive methods (and often differ by considerably less; note also that in these previous studies a smaller basis set was used, which may contribute to the observed errors).

To further put the uB3LYP results in perspective, the energies of structures **2–8** were computed at the uCCSD(T)/cc-pVDZ^{28a,b} level of theory, and separately, the geometries of these structures were optimized at the uMP2/6-31+G(d,p) level.^{28c} Unfortunately, both uMP2 and uCCSD(T) calculations suffered from significant spin contamination (~50%; see Supporting Information for details), diminishing the value of the results obtained with those methods. B3LYP calculations, however, suffered from only minor spin contamination (<10%). In general, variation of more than 20% in the spin expectation value is considered to be a serious problem. Also, counterintuitively, the CCSD(T) method predicts that allene–yne **2** has $\langle S^2 \rangle = 1.02$, which would indicate a diradical ground state. Consequently, we focus our discussion herein on the results of uB3LYP calculations, but uMP2 and uCCSD(T) results are collected in the Supporting Information. Efforts to carry out multireference computations^{28d} on the sorts of systems discussed herein will be described in a future report.

Results and Discussion

Concerted Considerations. To investigate the possibility of a concerted mechanism, a transition-state structure for the suprafacial/antarafacial cycloaddition of allene and acetylene was first located (Figure 2). This structure—although a computational artifact²⁹—does highlight the geometric requirements for such a process. An IRC calculation²⁴ shows the lowest energy pathway connecting the allene and ethyne to the cyclic diene product (blue trace, Figure 3). The red trace in Figure 3 shows the progression in the H3a–C3–C5–H5a dihedral angle as a function of the reaction coordinate, which varies from –40 to 125°, i.e., the terminal CH₂ group “flips over”, during the reactions, consistent with a suprafacial/antarafacial process, although the two bond-forming events occur very asynchronously.³⁰ To further illustrate this point, the C1–C4 bond distance was plotted against the C2–C3 bond distance over the course of this reaction in a More O’Ferrall–Jencks type plot (Figure 4).³¹ The red lines in this plot correspond to two different stepwise pathways, while a concerted synchronous pathway corresponds to the blue diagonal line. The asynchronous nature

- (20) To determine the magnitude of gas phase artifacts, structures **22–28** were optimized using the implicit solvent model CPCM with UAKS radii (with chlorobenzene as the solvent) and relative energetics were found to vary, in most cases, by less than 1 kcal/mol, indicating that the gas-phase approximation is reasonable in this case. (a) Yu, A.; Liu, Y.; Wang, Y. *Chem. Phys. Lett.* **2007**, *436*, 276–279. (b) Krol, M.; Wrona, M.; Page, C. S.; Bates, P. A. *J. Chem. Theory Comput.* **2006**, *2*, 1520–1529. (c) Takano, Y.; Houk, K. N. *J. Chem. Theory Comput.* **2005**, *1*, 70–77.
- (21) Frisch, M. J.; et al. GAUSSIAN03, Revision D.01; Gaussian, Inc.: Wallingford CT, 2004. See Supporting Information for complete citation.
- (22) (a) Lee, C.; Yang, W.; Parr, R. G. *Phys. Rev. B* **1988**, *37*, 785–789. (b) Becke, A. D. *J. Chem. Phys.* **1993**, *98*, 5648–5652. (c) Becke, A. D. *J. Chem. Phys.* **1993**, *98*, 1372–1377. (d) Stephens, P. J.; Devlin, F. J.; Chabalowski, C. F.; Frisch, M. J. *J. Phys. Chem.* **1994**, *98*, 11623–11627.
- (23) Single-point energy calculations at the mPW1PW91/6-31+G(d,p) level of theory were carried out on all structures to overcome a reported preference of B3LYP for acyclic structures; see: Matsuda, S. P. T.; Wilson, W. K.; Xiong, Q. *Org. Biomol. Chem.* **2006**, *4*, 530–543.
- (24) (a) Fukui, K. *Acc. Chem. Res.* **1981**, *14*, 363–368. (b) Gonzalez, C.; Schlegel, H. B. *J. Phys. Chem.* **1990**, *94*, 5523–5527.
- (25) Müller, N.; Falk, A. *Ball & Stick*, 4.0a12, Molecular graphics software for MacOS; Johannes Kepler University of Linz: Linz, Austria, 2004.
- (26) (a) Goldstein, E.; Beno, B.; Houk, K. N. *J. Am. Chem. Soc.* **1996**, *118*, 6036–6043. (b) Wittbrodt, J. M.; Schlegel, H. B. *J. Chem. Phys.* **1996**, *105*, 6574–6577. (c) Nendel, M.; Sperling, D.; Wiest, O.; Houk, K. N. *J. Org. Chem.* **2000**, *65*, 3259–3268. (d) Cremer, D.; Filatov, M.; Polo, V.; Kraka, E.; Shaik, S. *Int. J. Mol. Sci.* **2002**, *3*, 604–638. (e) Zhao, Y.-L.; Suhrada, C. P.; Jung, M. E.; Houk, K. N. *J. Am. Chem. Soc.* **2006**, *128*, 11106–11113. (f) Zhou, H.; Wong, N. B.; Lau, K. C.; Tian, A.; Li, W. K. *J. Phys. Chem. A* **2007**, *111*, 9838–9847. (g) Leach, A. G.; Houk, K. N.; Foote, C. S. *J. Org. Chem.* **2008**, *73*, 8511–8519.
- (27) (a) Abe, M.; Adam, W.; Borden, W. T.; Hattori, M.; Hrovat, D. A.; Nojima, M.; Nozaki, K.; Wirz, J. *J. Am. Chem. Soc.* **2003**, *126*, 574–582. (b) Zhang, D. Y.; Hrovat, D. A.; Abe, M.; Borden, W. T. *J. Am. Chem. Soc.* **2003**, *125*, 12823–12828. (c) Winter, A. H.; Falvey, D. E.; Cramer, C. J.; Gherman, B. F. *J. Am. Chem. Soc.* **2007**, *129*, 10113–10119.

- (28) (a) Raghavachari, K.; Trucks, G. W.; Pople, J. A.; Head-Gordon, M. *Chem. Phys. Lett.* **1989**, *157*, 479–483. (b) Dunning, T. H., Jr. *J. Chem. Phys.* **1989**, *90*, 1007–1023. (c) Möller, C.; Plesset, M. S. *Phys. Rev.* **1934**, *46*, 618–622. (d) Li, X.; Paldus, J. *J. Chem. Phys.* **2008**, *129*, 174101.
- (29) The wavefunction of this transition-state structure was determined to have an RHF-to-UHF instability, meaning that a diradical pathway is preferred.
- (30) Tantillo, D. J. *J. Phys. Org. Chem.* **2008**, *21*, 561–570.
- (31) (a) More O’Ferrall, R. A. *J. Chem. Soc. B* **1970**, 274–277. (b) Jencks, W. P. *Chem. Rev.* **1972**, *72*, 705–718.

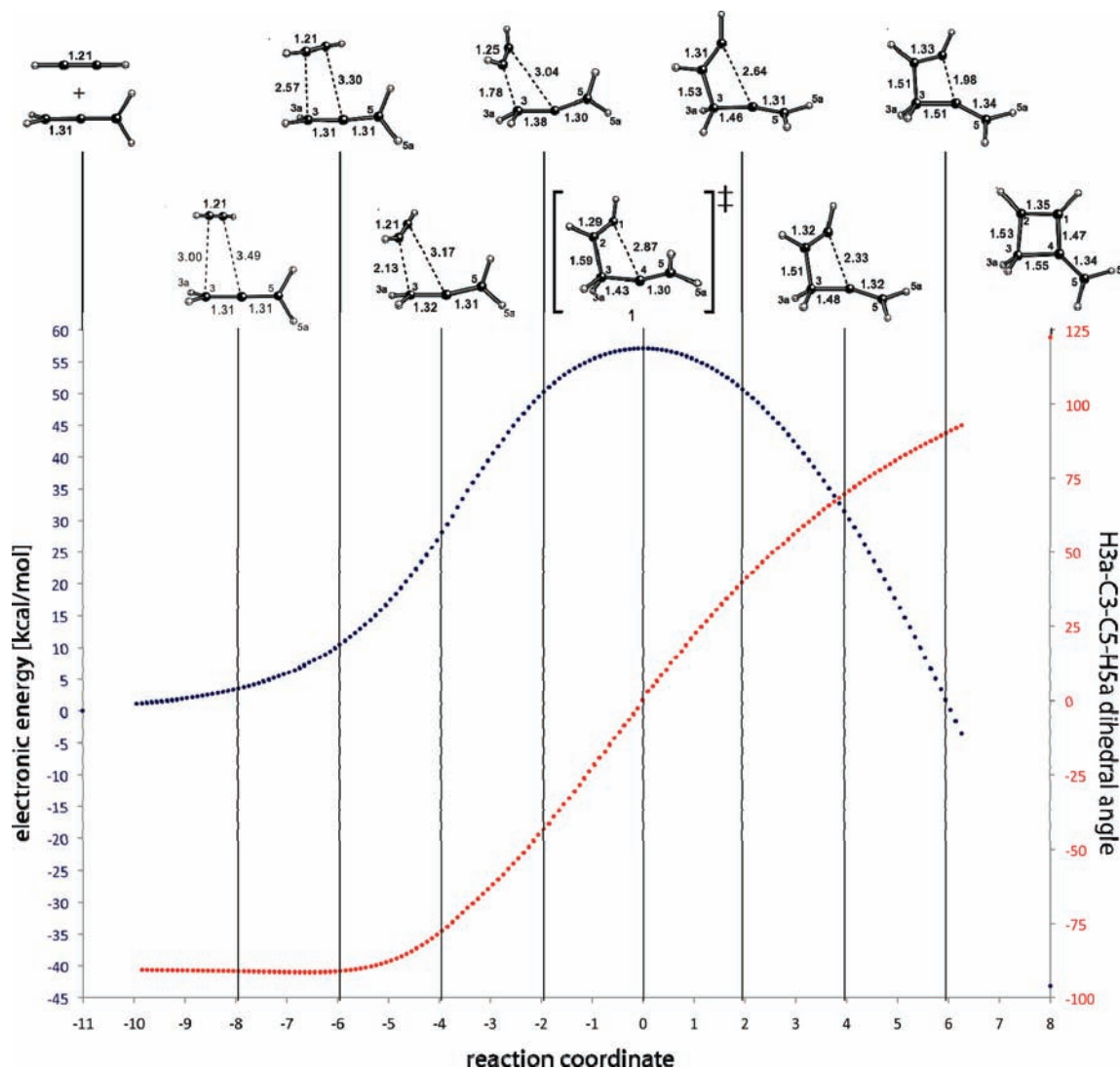


Figure 3. Energies (blue) and H3a–C3–C5–H5a dihedral (red) as a function of reaction coordinate for transition-state structure **1**, with select structures (at 20 point intervals from **1**) displayed. Select distances are shown in angstroms (Å), and electronic energies are relative to the isolated propa-1,2-diene and ethyne (at far left). Energies are reported without zero-point correction as no thermochemistry data is computed during the IRC calculation procedure.

of the two bond-forming events in the computed allene + acetylene reaction is clear from the deviation from the diagonal of the curve corresponding to points along the actual IRC (blue dots). The C2–C3 bond is largely formed before the C1–C4 bond forms to any significant extent (note that the IRC-based curve resides in the bottom right corner of the plot). Also of note is that the minimum energy pathway leaves the bounds of the red box; the C2–C3 distance proceeds to a short value and then lengthens slightly before arriving at the cyclobutene product. This final elongation may reflect a means of accommodating some of the ring strain associated with formation of the 4-membered ring.

The blue atoms in **1** (Figure 2) show the points at which a tether is attached in the synthetically examined systems (Figure 1). Notice that these attachment points are oriented in such a way that three methylenes will not suffice as a long enough chain to connect the two without severely distorting the core geometry of the transition-state structure. Given this observation, it is not surprising that we were unable to find a concerted pathway for the (tethered) systems described below.

Parent (Unsubstituted) Systems. The simplest of these tethered systems is hepta-1,2-dien-6-yne. Two stepwise diradical

cycloaddition mechanisms for this system are possible differing in whether a 5- or 7-membered ring is formed first (Scheme 1). The pathway involving initial 5-membered ring formation is shown in Figure 5. Even with allene–yne **2** preorganized for cyclization, a barrier of nearly 35 kcal/mol is found; this barrier is high, but could be surmounted under the experimental conditions (Figure 1). In the transition-state structure for this first cyclization step, the alkynyl group is starting to deviate from linearity, indicating that an alkenyl radical is forming. For the subsequent ring closure to occur, the alkenyl radical center must invert and point the bulk of its electron density toward the allyl radical with which it will combine. Inversion has a barrier of only a few kcal/mol. The resultant diradical, **6**, is capable of forming the 4-membered ring through a transition-state structure with a lower energy than that for the initial 5-membered ring formation. The bicyclic product, **8**, is lower in energy than its allene–yne precursor, despite the strain associated with accommodating a π -bond in a small ring. This strain is offset by the conversion of two C–C π -bonds to two C–C σ -bonds and the conjugation arising upon formation of the butadiene moiety.

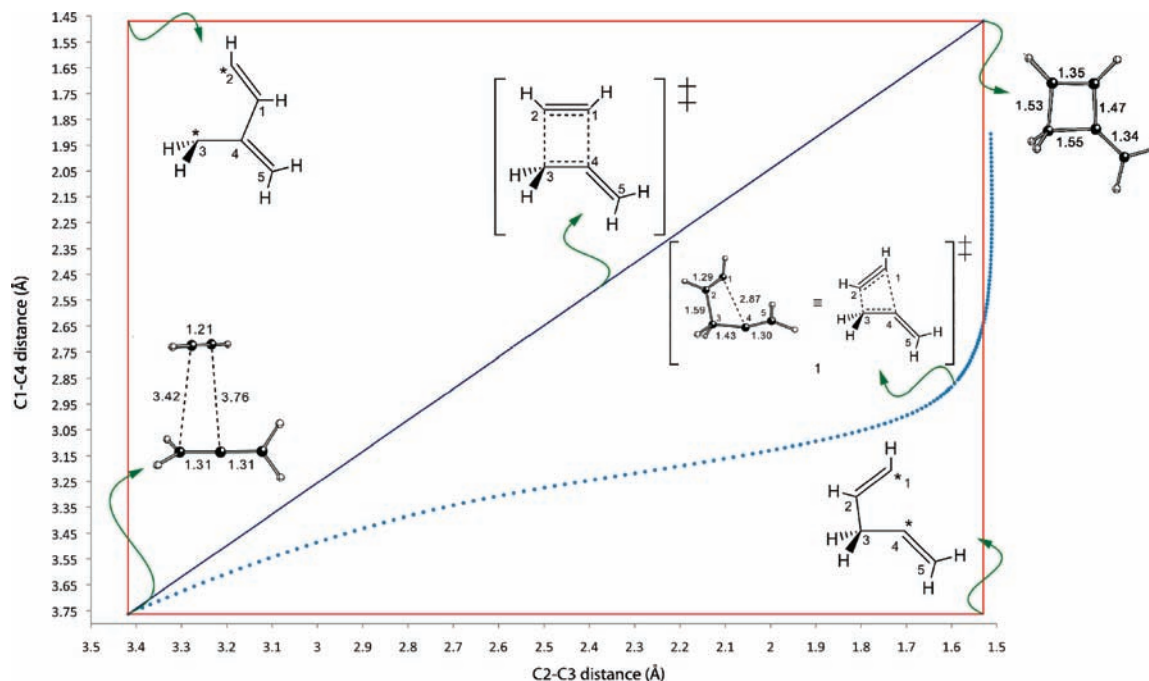


Figure 4. More O'Ferrall–Jencks plot illustrating the synchronicity of bond formation (C1–C4 and C2–C3) along the reaction coordinate. In proceeding from starting complex (lower left structure) to the product (top right structure) two possible stepwise pathways are shown (red) as well as a concerted synchronous pathway (solid blue line) and the pathway actually taken (blue data points derived from the IRC of Figure 3). Geometries of the starting complex (the last point of the IRC is not a stationary point), the transition-state structure, and the product are shown with select distances displayed in angstroms (Å).

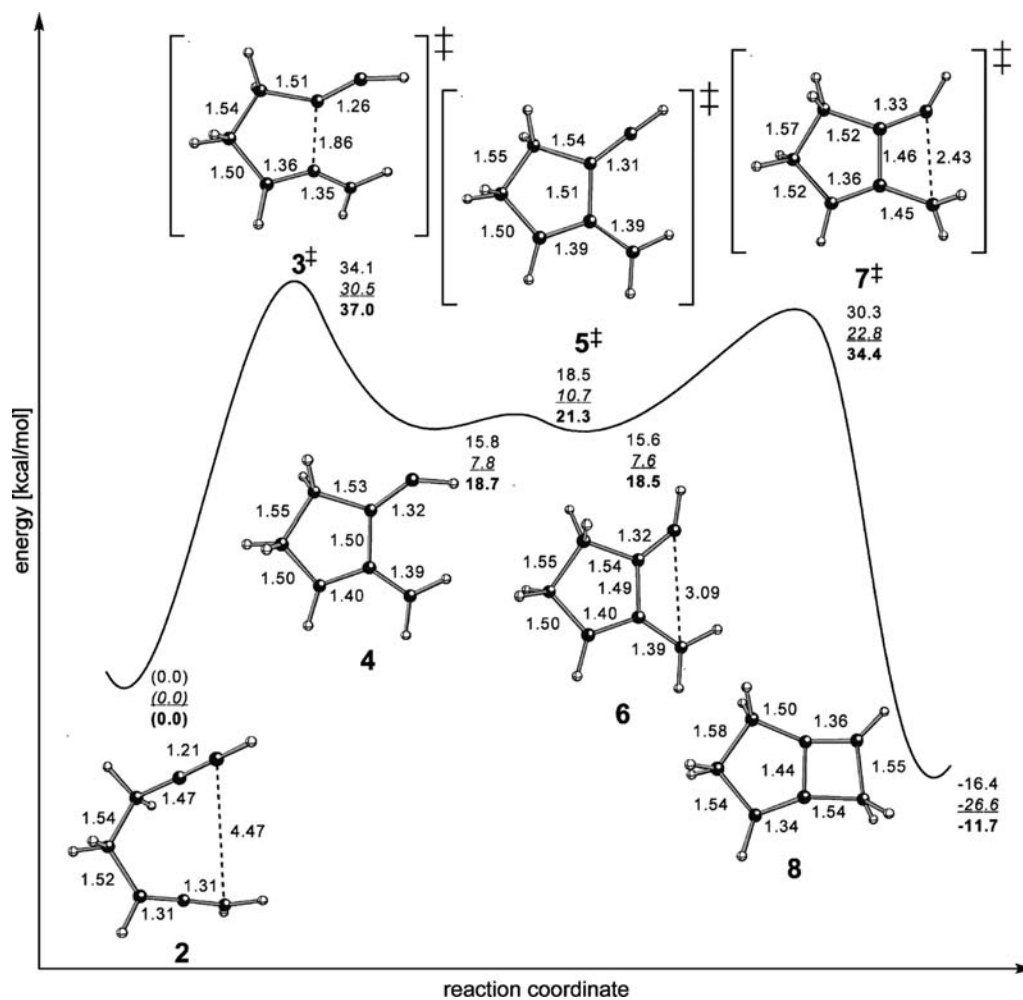


Figure 5. Pathway involving initial 5-membered ring formation for formal [2 + 2]-cycloaddition of hepta-1,2-diene-6-yne. Select distances are displayed in angstroms (Å), and zero-point corrected energies are also displayed, with results from B3LYP/6-31+G(d,p) calculations in normal text, those from mPW1PW91 in underlined italics, and Gibbs free energies at 250 °C in **bold**.

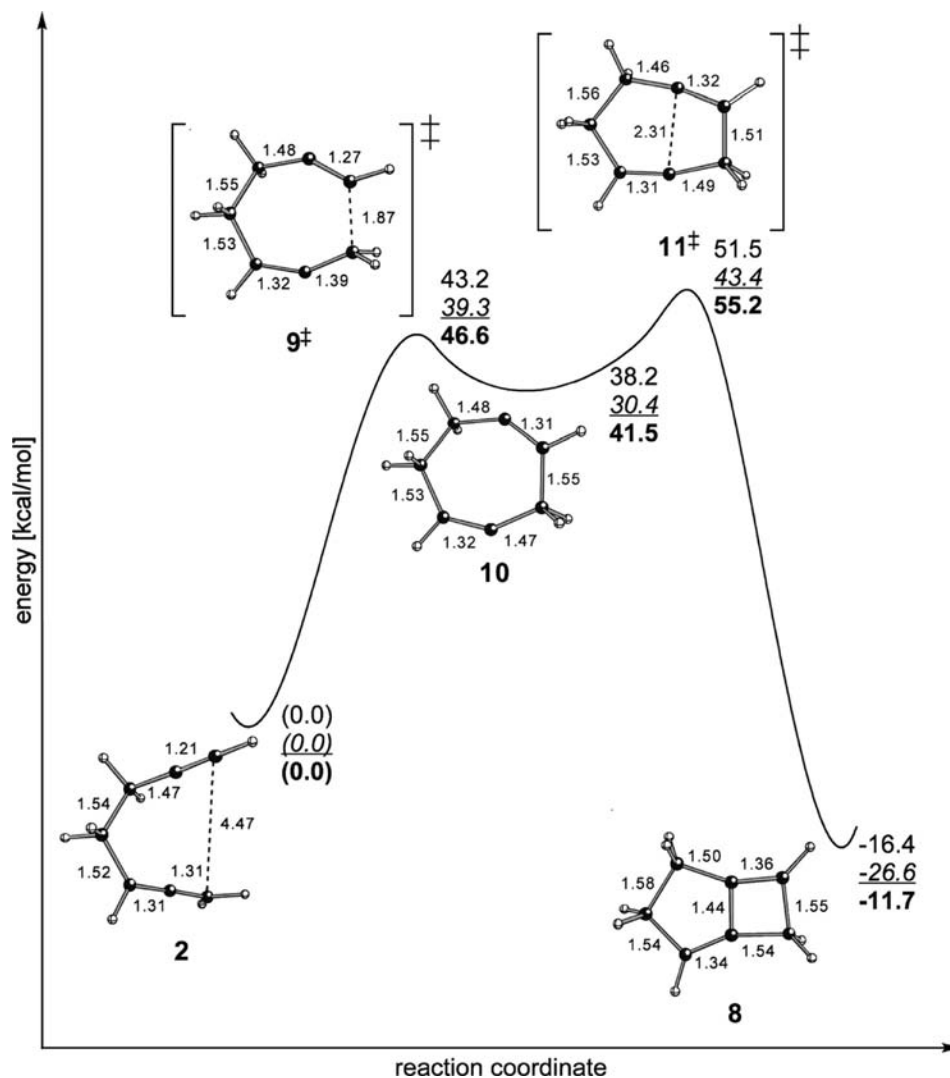


Figure 6. The pathway involving initial 7-membered ring formation for formal [2 + 2] cycloaddition of hepta-1,2-diene-6-yne. Select distances are displayed in angstroms (Å), and zero-point corrected Gibbs energies are also displayed, with results from B3LYP/6-31+G(d,p) calculations in normal text, those from mPW1PW91 in underlined italics, and Gibbs free energies at 250 °C in **bold**.

Formation of the C–C bonds in the opposite order is also a possibility. Such a pathway would involve initial formation of a 7-membered ring, followed by cyclization to form the fused 5–4 bicycle, as shown in Figure 6 (see also Scheme 1). The barrier for initial cyclization for this pathway is substantially higher than that for the pathway shown in Figure 5, likely a result of the fact that diradical **4** contains an allylic radical substructure, while intermediate **10** does not, and the associated delocalization is partly present in the transition-state structure for formation of **4**. The transition-state structure for the ultimate bond-forming step (**10**→**8**) is even higher in energy than that for the initial cyclization, and the overall barrier for this pathway is significantly higher than that for the pathway shown in Figure 5. Thus, forming the small ring first is favored by a considerable amount.

To determine the effect of tether length on the energetics of the favored pathway, systems analogous to that shown in Figure 5, but that form 6–, 7–, and 8–4 fused products, were examined. The energetic data for these systems are compiled

in Table 1 (see Supporting Information for geometries).³² The barriers for formation of the 5-, 6-, or 7-membered rings are all similar, while formation of an 8-membered ring is more difficult. A similar situation is observed for the other transition-state structures and intermediates, but larger differences are observed for the products. These results seem to indicate that a 7-membered ring is best at accommodating the diene substructure that is formed in the cycloaddition.

Regiochemical Preference. To probe the limits of the selectivity for reaction with the terminal π -bond of the allene, we return to the cyclization of octa-1,2-diene-7-yne. Interestingly, reaction with the internal π -bond prefers a mechanism in which the large ring is formed first (Figure 7; see Supporting Information for other pathway). This is again due to a preference for formation of an allyl radical substructure, which can only be achieved here if the large ring is formed first. The first bond-forming event is rate-limiting, and transition-state structure **13[‡]** is

(32) The pathway forming a large ring first was also computed for all systems; however, in every case that pathway had a substantially higher barrier. See Supporting Information for energetic data.

Table 1. Energetic Data^a for Systems with Different Tether Lengths³²

ring size	5	6	7	8
TS1	34.1	33.2	34.2	40.7
[kcal/mol]	<u>30.5</u>	<u>29.6</u>	<u>31.2</u>	<u>37.1</u>
	37.0	37.5	38.4	45.5
INT1	15.8	14.2	15.3	19.8
[kcal/mol]	<u>7.8</u>	<u>6.0</u>	<u>7.7</u>	<u>11.8</u>
	18.7	19.0	20.3	25.9
TS2	18.5	17.3	19.0	23.8
[kcal/mol]	<u>10.7</u>	<u>9.2</u>	<u>11.7</u>	<u>16.0</u>
	21.3	22.0	24.0	30.0
INT2	15.6	13.6	15.3	20.1
[kcal/mol]	<u>7.6</u>	<u>5.4</u>	<u>7.8</u>	<u>12.2</u>
	18.5	18.4	20.3	26.3
TS3	30.3	20.6	19.9	27.7
[kcal/mol]	<u>22.8</u>	<u>13.1</u>	<u>12.8</u>	<u>20.2</u>
	34.4	26.6	26.1	35.2
PR	-16.4	-32.3	-38.4	-31.3
[kcal/mol]	<u>-26.6</u>	<u>-42.7</u>	<u>-48.3</u>	<u>-41.7</u>
	-11.7	-25.7	-31.6	-24.0

^a Zero-point corrected energies are displayed, with results from B3LYP/6-31+G(d,p) calculations in normal text, those from mPW1PW91 in underlined italics, and Gibbs free energies at 250 °C in **bold**.

approximately 3 kcal/mol higher in energy than the rate-limiting transition-state structure for reaction with the terminal π -bond of the allene (compare Figure 7 with Table 1, ring size = 6), consistent with the experimentally observed selectivity (Figure 1).

Substituted Systems with a Terminal Allene. Next, the effects of substituents on the energetics of this [2 + 2] cycloaddition reaction were examined. The system shown in Figure 1c bears carbonyl and phenyl substituents, and we wanted to know whether these groups play an important role in stabilizing intermediates and/or transition-state structures. Figure 8 shows the cycloaddition that forms a 6–4 fused product with both phenyl and carbonyl substituents. In this case, there is only a single intermediate while two were found earlier (compare Figures 5 and 8). The barrier of 30–35 kcal/mol seems to be in reasonable agreement with the experimental observation of a reaction temperature of 250 °C.¹¹

In order to determine which substituent was responsible for this difference and also how each substituent affects the energetics for rearrangement, systems lacking one or the other were examined; the results of these calculations are summarized in Table 2 (see Supporting Information for geometries). Comparison of the substituent-free and carbonyl-substituted systems (the first two columns

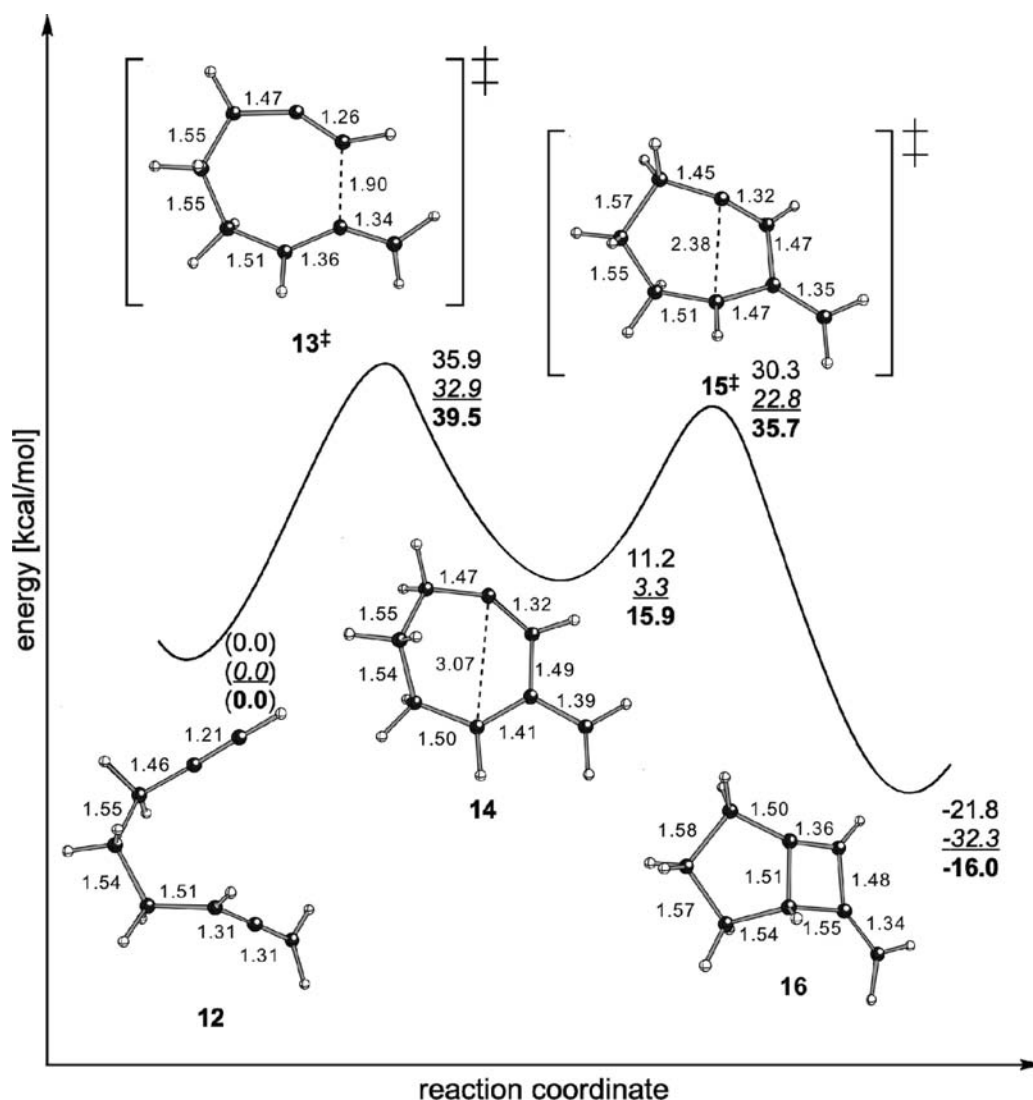


Figure 7. Alternative [2 + 2] cycloaddition for octa-1,2-diene-7-yne to form a 5–4 fused product. Select distances are displayed in angstroms (Å), and zero-point corrected energies are also displayed, with results from B3LYP/6-31+G(d,p) calculations in normal text, those from mPW1PW91 in underlined italics, and Gibbs free energies at 250 °C in **bold**.

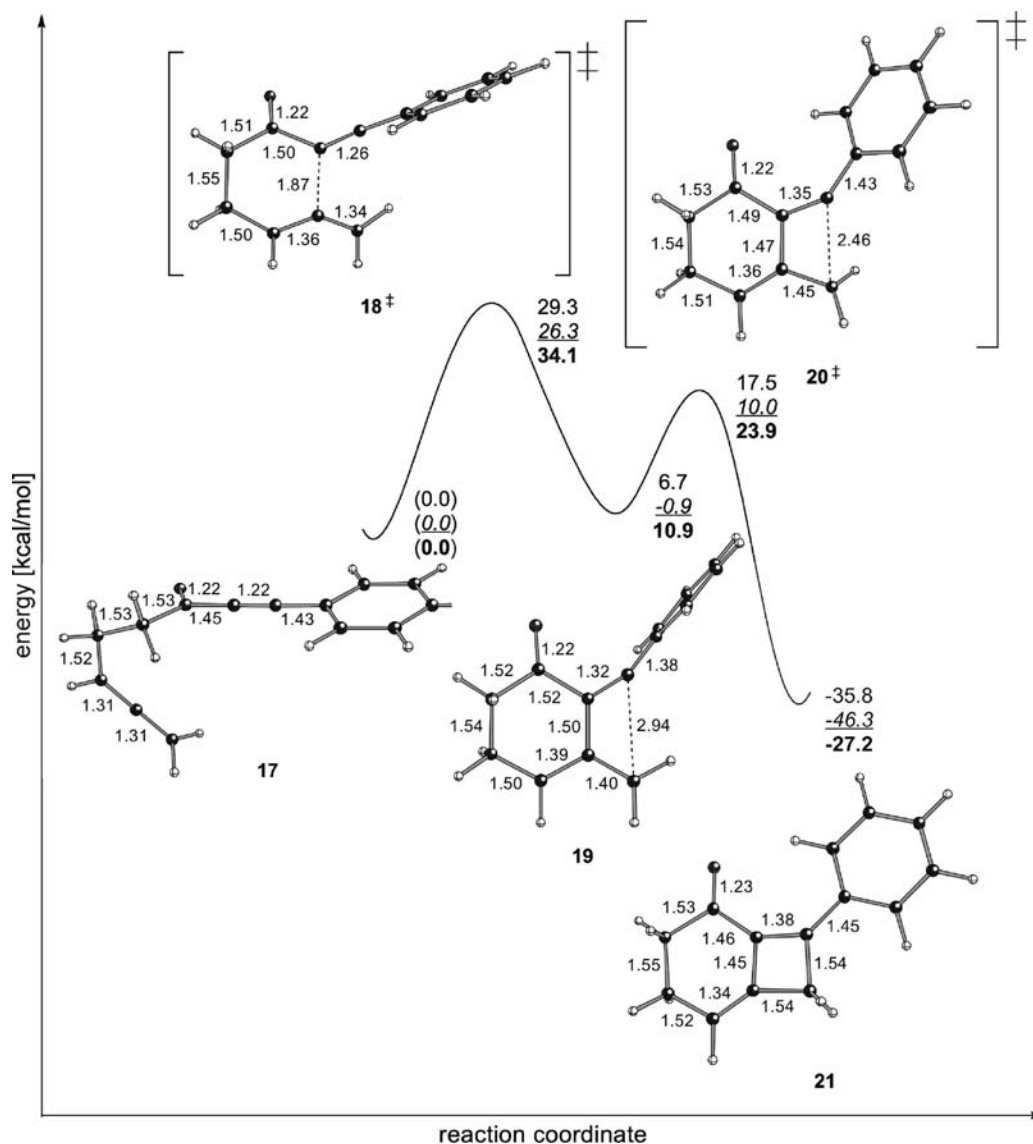


Figure 8. Formal [2 + 2] cycloaddition to form a 6–4 fused product with both phenyl and carbonyl substituents. Select distances are displayed in angstroms (Å), and zero-point corrected energies are also displayed, with results from B3LYP/6-31+G(d,p) calculations in normal text, those from mPW1PW91 in *underlined italics*, and Gibbs free energies at 250 °C in **bold**.

Table 2. Energetic Data^a for Systems Bearing Different Substituents³²

substituent	none	carbonyl	phenyl	carbonyl and phenyl
TS1	33.2	33.5	28.5	29.3
[kcal/mol]	<u>29.6</u>	<u>30.1</u>	<u>25.3</u>	<u>26.3</u>
	37.5	37.3	35.4	34.1
INT1	14.2	13.3	7.1	6.7
[kcal/mol]	<u>6.0</u>	<u>4.8</u>	<u>-0.4</u>	<u>-0.9</u>
	19.0	17.6	13.3	10.9
TS2	17.3	15.6	—	—
[kcal/mol]	<u>9.2</u>	<u>7.3</u>	—	—
	22.0	19.8	—	—
INT2	13.6	11.1	—	—
[kcal/mol]	<u>5.4</u>	<u>2.6</u>	—	—
	18.4	15.1	—	—
TS3	20.6	19.7	16.4	17.5
[kcal/mol]	<u>13.1</u>	<u>12.2</u>	<u>9.1</u>	<u>10.0</u>
	26.6	25.4	24.4	23.9
PR	-32.3	-33.9	-33.6	-35.8
[kcal/mol]	<u>-42.7</u>	<u>-44.0</u>	<u>-44.2</u>	<u>-46.3</u>
	-25.7	-27.4	-23.9	-27.2

^a Zero-point corrected energies are displayed with results from B3LYP/6-31+G(d,p) calculations appearing in normal text, those from mPW1PW91 appear in *underlined italics*, and **bold** energies are Gibbs free energies at 250 °C.

of Table 2) reveals that the carbonyl substituent has only a small effect on the energetics, providing slight stabilization of most structures relative to reactants, and two diradical intermediates are still involved in the rearrangement. In contrast, for the phenyl-substituted system, again only a single intermediate is observed. This system has radical character at the benzylic position, allowing for delocalization into the phenyl ring, which is manifested in a nearly linear geometry at this site and a significantly lower energy for this intermediate (relative to that of its reactant) compared to the intermediates in systems without the phenyl group (Tables 1 and 2).

The presence of a diradical intermediate could, in principle, be observed experimentally. Cyclopropyl radicals are known to undergo a ring-fragmentation process with very predictable rates.³³ For this reason we investigated the mechanistic pathway for a cyclopropyl substituted allene–yne; the computational results for the initial step appear in Figure 9 and indicate that the barrier for diradical formation is not significantly affected by this substituent.

(33) (a) Newcomb, M. *Tetrahedron* **1993**, *49*, 1151–1176. (b) Nonhebel, D. C. *Chem. Soc. Rev.* **1993**, *22*, 347–359.

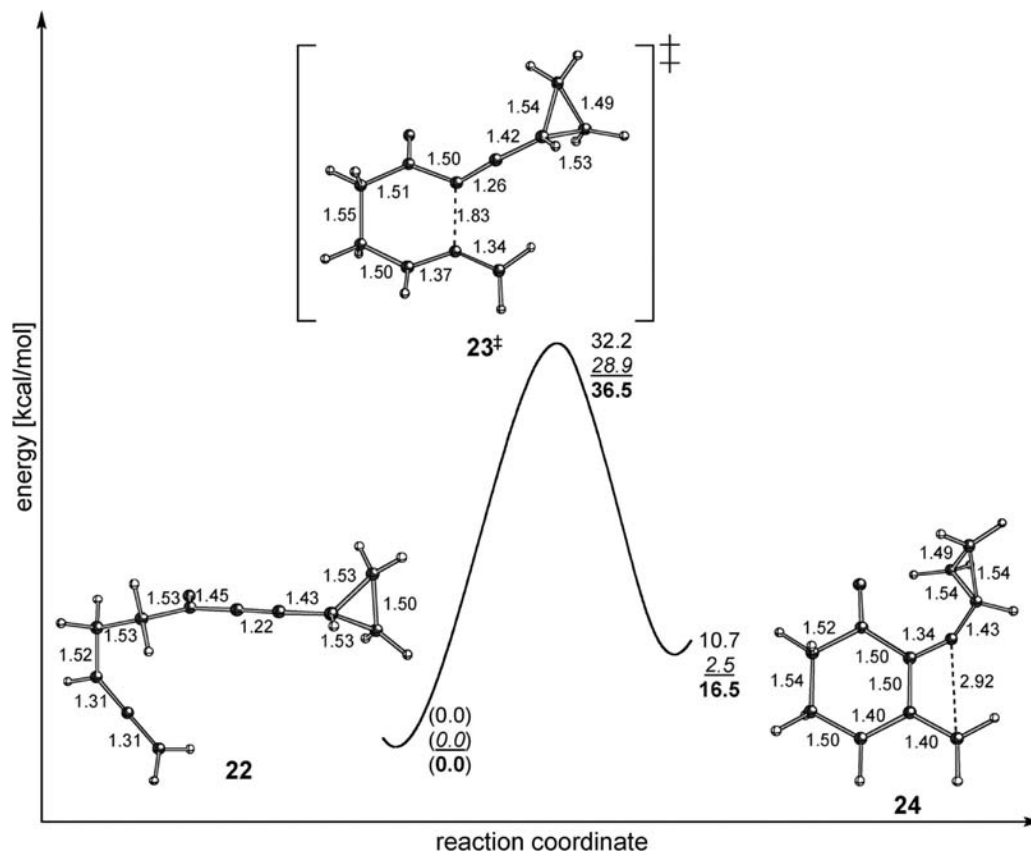


Figure 9. Initial step of the [2 + 2] cycloaddition for a carbonyl and cyclopropane substituted octa-1,5-diene-7-yne that forms a 6–4 fused product. Select distances are displayed in angstroms (Å), and zero-point corrected energies are also displayed, with results from B3LYP/6-31+G(d,p) calculations in normal text, those from mPW1PW91 in *underlined italics*, and Gibbs free energies at 250 °C in **bold**.

The formation of the 4-membered ring is shown in Figure 10 (**24** → **26**). As observed for the phenyl substituted system (Figure 8), only one intermediate (**24**) spans the two ring-closing transition structures. It is also worth noting that the second ring-closing step (via **25**[‡]) is similar to that for the carbonyl and phenyl substituted system. Figure 10 also depicts the cyclopropane ring-opening step (via **27**[‡]), which happens to be kinetically competitive with the second ring closure (transition structure energies of 18.3 kcal/mol for **27**[‡] and 18.6 kcal/mol for **25**[‡]).

In an attempt to determine whether solvent may have any effect on the mechanism, the structures in Figures 9 and 10 were recomputed in chlorobenzene (experimentally *o*-dichlorobenzene is used) and the results appear in Table 3 (also compiled in the table are energetics for diphenyl substituted **22**–**28**; *vide infra*). It is clear from the difference in energy (between gas- and solution-phase) for each structure, that the solvent has very little effect (the biggest difference in energies is 1.2 kcal/mol).

Probing the Formation of a Thermally Generated Biradical Intermediate Experimentally.³⁴ In an effort to probe the formation of the biradical intermediates predicted *in silico*, a series of intramolecular radical-trapping experiments were conducted, and the results of these studies are reported below. Investigation of the thermal [2 + 2] cycloaddition reaction of allene–ynes using radical clock probes began by using cyclopropyl derivatives,

which have been used extensively as radical clocks and mechanistic probes.³⁵ Consequently, substantial data are available; however, the literature provides minimal data on the behavior of vinyl and allyl radicals.³⁶ The disadvantage to using such a radical probe in this cycloaddition reaction is the lack of a clear kinetic preference for ring-opening (e.g., Figure 10), and dynamic effects,³⁷ which would presumably favor cyclobutene ring-closing over cyclopropane ring-opening. Thus, several probe substrates were designed, synthesized, and tested

(34) The possibility of a photochemically initiated [2 + 2] cycloaddition reaction was explored using 1-phenylocta-6,7-dien-1-yn-3-one. The substrate was subjected to light emitting in the range of its absorbance frequency (280 nm) for 2 h. No reaction occurred, and the starting material was completely recovered.

- (35) (a) Newcomb, M.; Johnson, C. C.; Manek, M. B.; Varick, T. R. *J. Am. Chem. Soc.* **1992**, *114*, 10915–10921. (b) Adam, W.; Curci, R.; D'Accolti, L.; Dinioi, A.; Fusco, C.; Gasparrini, F.; Kluge, R.; Paredes, R.; Schulz, M.; Smerz, A. K.; Veloza, L. A.; Weinkötz, S.; Winde, R. *Chem.–Eur. J.* **1997**, *3*, 105–109. (c) Roubelakis, M. M.; Vougioukalakis, G. C.; Angelis, Y. S.; Orfanopoulos, M. *Org. Lett.* **2005**, *8*, 39–42. (d) Schmittel, M.; Mahajan, A. A.; Bucher, G. t.; Bats, J. W. *J. Org. Chem.* **2007**, *72*, 2166–2173. (e) Bucher, G.; Mahajan, A. A.; Schmittel, M. *J. Org. Chem.* **2009**, *74*, 5850–5860. (36) (a) Crandall, J. K.; Tindell, G. L.; Manmade, A. *Tetrahedron Lett.* **1982**, *23*, 3769–3772. (b) Back, T. G.; Muralidharan, K. R. *J. Org. Chem.* **1989**, *54*, 121–125. (c) Mainetti, E.; Fensterbank, L.; Malacria, M. *Synlett* **2002**, *6*, 923–926. (d) Milnes, K. K.; Gottschling, S. E.; Baines, K. M. *Org. Biomol. Chem.* **2004**, *2*, 3530–3534. (e) Gottschling, S. E.; Grant, T. N.; Milnes, K. K.; Jennings, M. C.; Baines, K. M. *J. Org. Chem.* **2005**, *70*, 2686–2695. (37) For leading references on non-statistical dynamic effects in organic chemistry see: (a) Carpenter, B. K. *Acc. Chem. Res.* **1992**, *25*, 520–528. (b) Carpenter, B. K. *Angew. Chem., Int. Ed.* **1998**, *37*, 3340–3350. (c) Bachrach, S. M.; Gilbert, J. C. *J. Org. Chem.* **2004**, *69*, 6357–6364. (d) Carpenter, B. K. *Annu. Rev. Phys. Chem.* **2005**, *56*, 57–89. (e) Ussing, B. R.; Hang, C.; Singleton, D. A. *J. Am. Chem. Soc.* **2006**, *128*, 7594–7607. (f) Thomas, J. B.; Waas, J. R.; Harmata, M.; Singleton, D. A. *J. Am. Chem. Soc.* **2008**, *130*, 14544–14555. (g) Glowacki, D. R.; Marsden, S. P.; Pilling, M. J. *J. Am. Chem. Soc.* **2009**, *131*, 13896–13897.

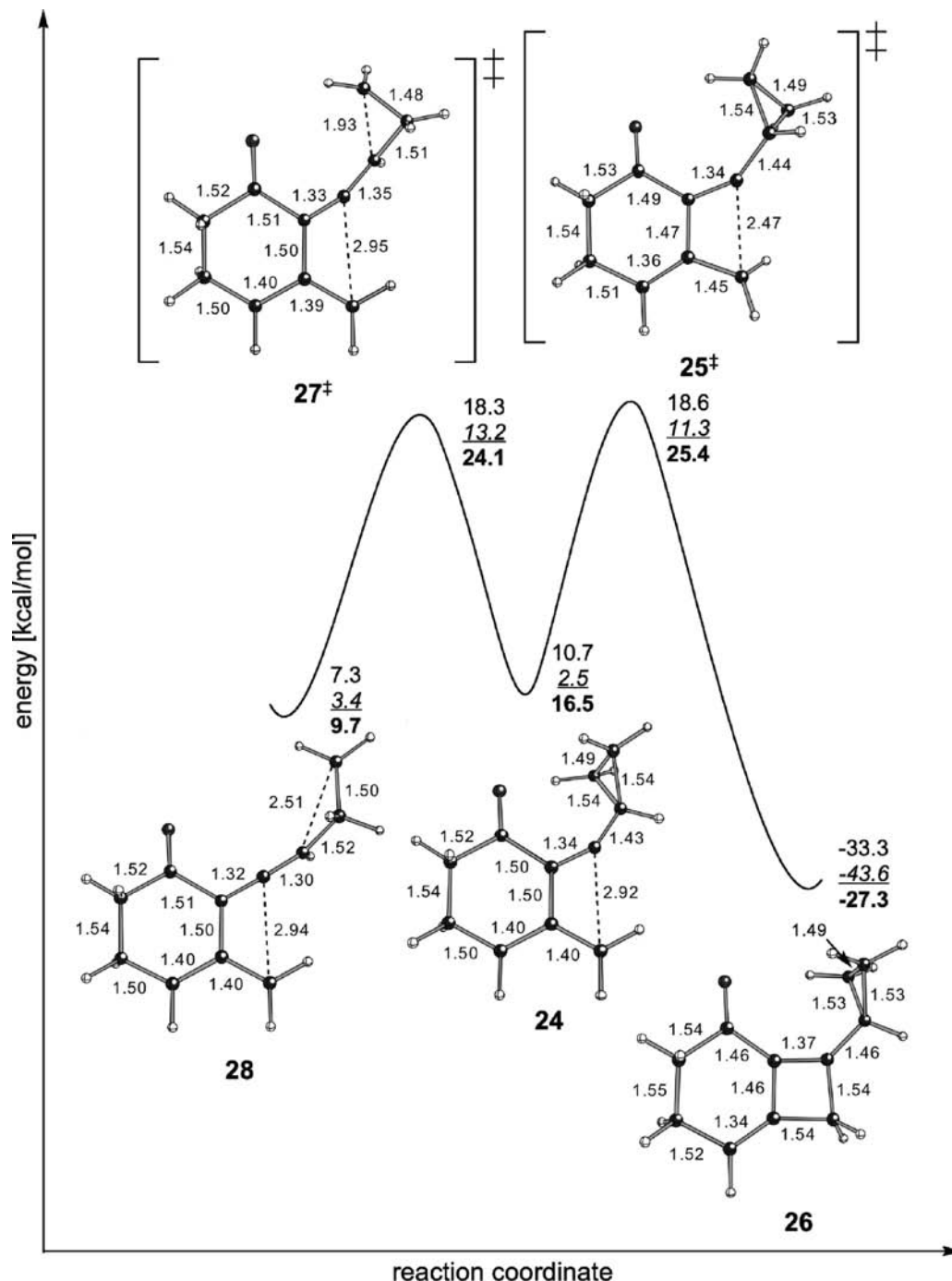


Figure 10. Divergent pathways for net [2 + 2]-cycloaddition and cyclopropyl ring-opening for a carbonyl and cyclopropane substituted octa-1,2-diene-7-yne that forms a 6–4 fused product. Select distances are displayed in angstroms (Å), and zero-point corrected energies are also displayed, with results from B3LYP/6-31+G(d,p) calculations in normal text, those from mPW1PW91 in *underlined italics*, and Gibbs free energies at 250 °C in bold.

in an effort to (1) gather evidence for the postulated biradical intermediate and (2) determine whether the biradical could function as an initiating point for radical cascade reactions.

Two series of substrates were chosen to look at the mechanism of the thermally promoted [2 + 2] cycloaddition of an allene–yne: series A (Figure 11, **29–31**) possessing the cyclopropyl group on the terminus of the allene; and series B (Figure 11, **22, 32, 33**) possessing the cyclopropyl group on the terminus of the alkyne. Within each series, the substituents on the cyclopropyl group are modified from all hydrogen containing to a 1,1-diphenylcyclopropyl and 1-methoxy-2-phenylcyclopropyl. The simple cyclopropyl group was chosen

due to it being less likely to undergo spontaneous ring-opening in the absence of a radical intermediate. The diphenylcyclopropyl group undergoes a much faster ring-opening than the parent cyclopropane, and the 1-methoxy-2-phenylcyclopropyl is a probe used to distinguish between radicals and cations.³⁸

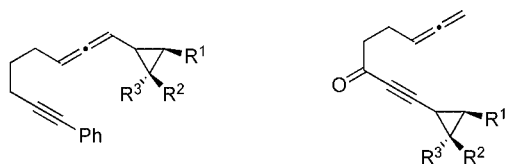
The preparation of these two series of compounds is depicted in Scheme 2. Synthesis of compound **29** was accomplished by

(38) (a) Newcomb, M.; Chestney, D. L. *J. Am. Chem. Soc.* **1994**, *116*, 9753–9754. (b) Newcomb, M.; Le Tadic-Biadatti, M.-H.; Chestney, D. L.; Roberts, E. S.; Hollenberg, P. F. *J. Am. Chem. Soc.* **1995**, *117*, 12085–12091. (c) Le Tadic-Biadatti, M.-H.; Newcomb, M. *J. Chem. Soc., Perkin Trans. 2* **1996**, 1467–1473.

Table 3. Energetic Data^a for Structures in Figures 9 and 10 in the Gas-Phase, Solution (Chlorobenzene)-Phase, and the Gas-Phase *gem*-Diphenylcyclopropane Substituted Systems

structure	none	none (solvent)	diphenyl
23 [‡]	32.2	32.4	32.5
	<u>28.9</u>	<u>29.1</u>	<u>29.1</u>
	36.5	36.6	36.6
24	10.7	11.9	10.7
	<u>2.5</u>	<u>3.7</u>	<u>2.6</u>
	16.5	17.2	15.9
25 [‡]	18.6	19.7	16.5
	<u>11.3</u>	<u>12.4</u>	<u>8.8</u>
	25.4	26.2	24.3
26	-33.3	-32.6	-33.2
	<u>-43.6</u>	<u>-43.0</u>	<u>-43.8</u>
	-27.3	-26.8	-24.2
27 [‡]	18.3	19.0	13.6
	<u>13.2</u>	<u>13.8</u>	<u>7.1</u>
	24.1	24.5	20.1
28	7.3	7.5	-7.4
	<u>3.4</u>	<u>3.6</u>	<u>-11.1</u>
	9.7	9.7	-2.9

^a Zero-point corrected energies are displayed with results from B3LYP/6-31+G(d,p) calculations appearing in normal text, those from mPW1PW91 appear in underlined italics, and **bold** energies are Gibbs free energies at 250 °C.



Series A

29 R¹ = R² = R³ = H

30 R¹ = H, R² = R³ = Ph

31 R¹ = OMe, R² = Ph, R³ = H

Series B

22 R¹ = R² = R³ = H

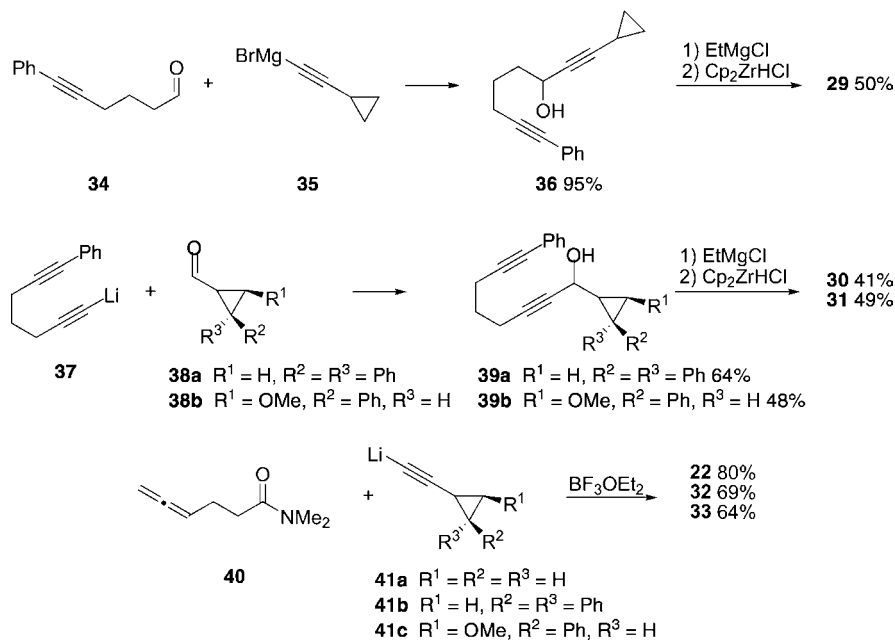
32 R¹ = H, R² = R³ = Ph

33 R¹ = OMe, R² = Ph, R³ = H

Figure 11. Substrates prepared to probe the mechanism of the thermal allene–yne [2 + 2] cycloaddition reaction.

the addition of cyclopropyl Grignard reagent **35** to aldehyde **34** giving propargylic alcohol **36** in 95% yield. Subjecting **36** to the Ready and Pu allene forming protocol provided allene–yne

Scheme 2. Preparation of the Substrates Used To Explore the Mechanism of the Thermal Allene–Yne [2 + 2] Cycloaddition Reaction

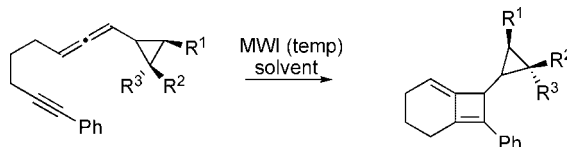


29 in 50% yield.³⁹ Similarly the lithium anion **37** was added to aldehyde **38a** affording alcohol **39a** in 64% yield. Propargylic alcohol **39a** was converted to allene–yne **30** in 41% yield upon exposure to the hydrozirconation conditions. Allene–yne **31** was prepared in an analogous manner to **30** using aldehyde **38b**. The B series of compounds **22**, **32**, and **33** were all prepared by the addition of the lithium acetylide **41a**, **41b**, or **41c** to amide **40**.

The results of heating the compounds in series A and B in the microwave are depicted in Tables 4 and 5. Heating **29** in deuterated *o*-dichlorobenzene for 30 min at 225 °C gave an 83% yield of the [2 + 2] cycloaddition product **42** (Table 4, entry 1). The product was not chromatographically stable so the yield was determined on the basis of ¹H NMR. Similar results were seen when heating **31**, only the reaction temperature was lower due to decomposition observed in the model system at higher temperatures.⁴⁰ Heating the diphenyl-substituted cyclopropane **30** gave only trace quantities of the [2 + 2] cycloadduct and a number of other compounds by crude NMR. The compounds were inseparable by column chromatography, and efforts to achieve separation by HPLC were unsuccessful.

Reaction of **22** under the standard microwave conditions also gave the [2 + 2] cycloadduct in 66% yield (Table 5, entry 1). The stability of compound **26** was a problem so the yield was determined by ¹H NMR.

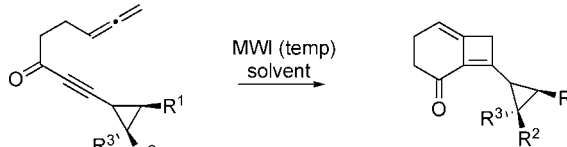
In the case of **32**, upon heating to 225 °C for 45 min, compounds **47** and **48** (Scheme 3) were isolated as isomers at the terminus of the exocyclic double bond of the cyclobutene. It is postulated that the formation of this product occurs via the initial formation of the diradical **49** followed by a radical-initiated ring-opening of the vinyl cyclopropane to give **50**. Rearrangement of the diradical in **50** leads to the formation of compound **51**. Upon electrocyclization of the alkene and allene in **51**, trienes **47** and **48** are produced in 20% and 24% yield, respectively.⁴¹ Although an alternative mechanism, whereby the [2 + 2] cycloaddition occurs to give the usual alkylidene cyclobutene followed by the spontaneous ring-opening of the diphenylcyclopropane **45** could, in principle, lead to the same

Table 4. Microwave Irradiation of Allene–Ynes **29–31**


entry	allene–yne	solvent	temp (°C) ^a /time (min)	yield (cmpd, %)
1	R ¹ = R ² = R ³ = H, 29	DCB-d ₄ ^b	225/30	42 83% ^c
2	R ¹ = H, R ² = R ³ = Ph, 30	BTF ^d	180/50	43 trace ^e
3	R ¹ = OMe, R ² = Ph, R ³ = H, 31	DCB ^b	180/60	44 85% ^c

42 R¹ = R² = R³ = H
43 R¹ = H, R² = R³ = Ph
44 R¹ = OMe, R² = Ph, R³ = H

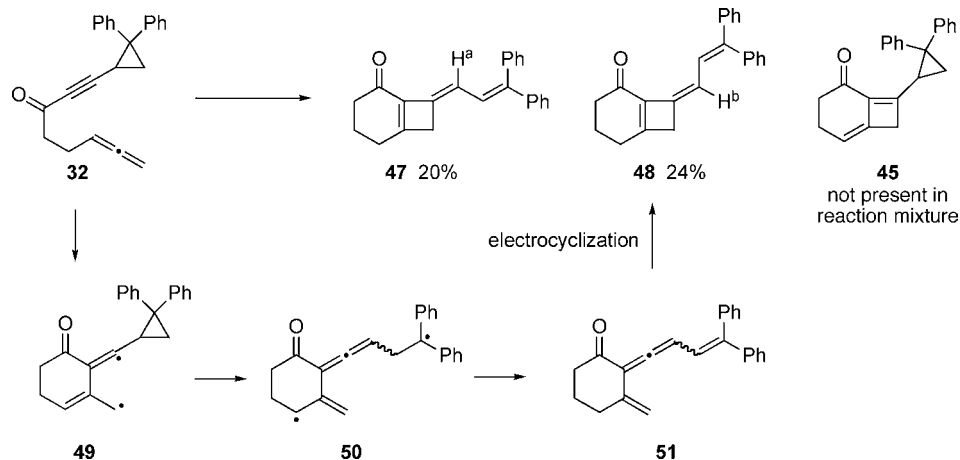
^a The reaction temperatures were chosen on the basis of tolerated conditions of control experiments that were performed using a model system (see Supporting Information). Temperatures lower than 180 °C resulted in unacceptably long microwave reaction times with the inability to obtain complete consumption of starting material. ^b DCB = *o*-dichlorobenzene. ^c Yield was determined by ¹H NMR. ^d BTF = benzonotrifluoride. ^e Based on crude ¹H NMR, a small amount of [2 + 2] adduct was formed; however, the majority of the material was composed of inseparable and unidentified compounds.

Table 5. Microwave Irradiation of Allene–Ynes **22, 32, and 33**


entry	allene–yne	solvent ^a	temp (°C)/time (min)	yield (cmpd, %)
1	R ¹ = R ² = R ³ = H, 22	DCB-d ₄ ^b	225/30	26 66% ^c
2	R ¹ = H, R ² = R ³ = Ph, 32	DCB ^b	225/45	45 0% ^d
3	R ¹ = OMe, R ² = Ph, R ³ = H, 33	DCB ^b	225/40	46 0% ^d

26 R¹ = R² = R³ = H
45 R¹ = H, R² = R³ = Ph
46 R¹ = OMe, R² = Ph, R³ = H

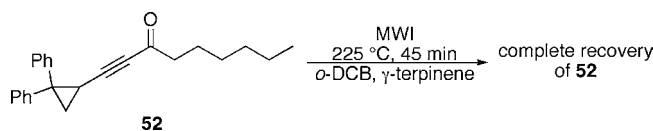
^a In all reactions, 150 equiv of γ -terpinene was added to the reaction mixture. In the absence of γ -terpinene, the reactions of **32** and **33** each resulted in a complex mixture of products. ^b DCB = *o*-dichlorobenzene; ^c Yield is based on ¹H NMR; ^d No [2 + 2] adduct was isolated; however, new products did form and are discussed below.

Scheme 3. Proposed Mechanism for the Formation of Trienes **47** and **48**^{a, 42}

^a The stereochemistry of **47** and **48** was not assigned experimentally, but was assigned by comparison of the experimental spectra to the spectra predicted by Spartan '08 (see Supporting Information).

products, the observation of **47** and **48** prompted us to examine other systems.

A control experiment was performed where 1-(2,2-diphenylcyclopropyl)non-1-yn-3-one (**52**, Figure 12) was heated under

**Figure 12.** Control experiment to ensure the diphenylcyclopropane does not open under the reaction conditions.

the same conditions as allene–ynone **32** (225 °C, *o*-DCB, γ -terpinene, 45 min) and the starting material was recovered unchanged in quantitative yield, although there may be added incentive for ring-opening from the [2 + 2] cycloadduct **45**.

(39) Pu, X.; Ready, J. M. *J. Am. Chem. Soc.* **2008**, *130*, 10874–10875.

(40) For each cyclopropyl substrate explored, a control substrate containing the cyclopropane appended to the allene or alkyne, but not containing the tethered alkyne or allene was prepared and subjected to the reaction conditions (See Supporting Information).

(41) For an example of a synthetically useful allene-ene electrocyclization see: Murakami, M.; Ashida, S.; Matsuda, T. *J. Am. Chem. Soc.* **2004**, *126*, 10838–10839.(42) *Spartan '08*; Wavefunction, Inc.: Irvine, CA, 2008.

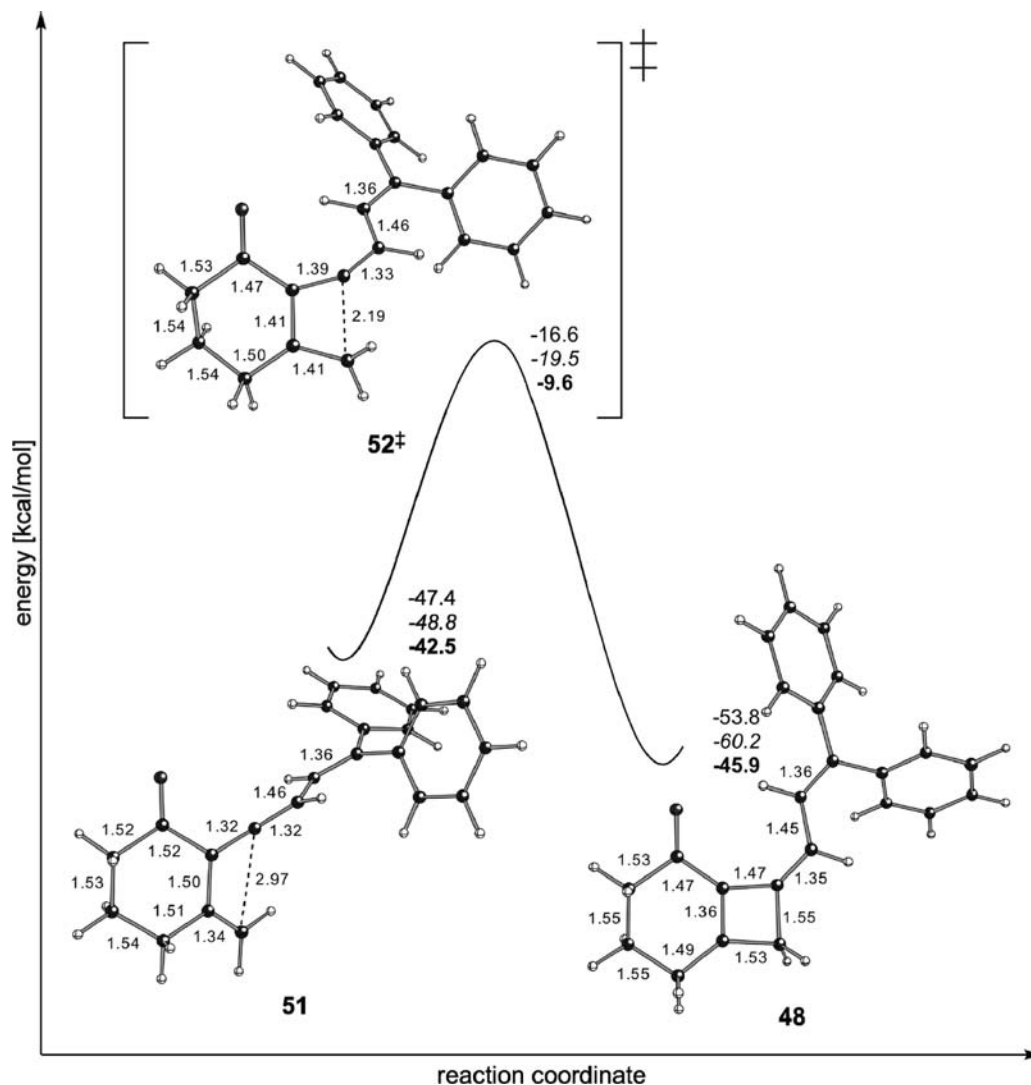


Figure 13. 4 π -Electrocyclic ring closure producing the experimentally observed product from the purported intermediate (derived from cyclopropane ring fragmentation from the *gem*-diphenylcyclopropane substituted octa-1,2-diene-7-yne). Select distances are displayed in angstroms (Å), and zero-point corrected energies are also displayed on the same scale as Table 3 (diphenyl column), with results from B3LYP/6-31+G(d,p) calculations in normal text, those from mPW1PW91 in *underlined italics*, and Gibbs free energies at 250 °C in **bold**.

Efforts to prepare the alkylidene cyclobutene **45** via alternative routes have not been successful.

Conversion of **32** to **49** (and subsequently to **45** and **50**) is described computationally in the column labeled "diphenyl" in Table 3. Note that addition of the two phenyl substituents to the cyclopropane ring increases the preference for ring-opening (**27[‡]**; as compared to cyclobutane ring-closing, **25[‡]**) from 0.3–1.9 kcal/mol (unsubstituted cyclopropane) to 1.7–4.2 kcal/mol (diphenyl substituted). The barrier for the 4 π -electrocyclic ring closure converting **51** to **48** was investigated computationally; those results appear in Figure 13. The first feature of note is that the starting allene **51** is nearly 50 kcal/mol lower in energy than its allene-ynone precursor and is approximately 5–10 kcal/mol lower than its bicyclic precursor (**26**, diphenyl, Table 3). This thermodynamic preference is consistent with the generation of the allene intermediate **51**, especially under such a high temperature (225 °C; Table 5, entry 2). We can draw further information from Figure 13, including the fact that the barrier (approximately 20–30 kcal/mol) is no higher than that for the initial cyclization step (**23[‡]**, diphenyl, Table 3). Lastly, the product of electrocyclization **48** is lower in energy than its allene precursor **51**—the reaction to form a fused 6–4 ring

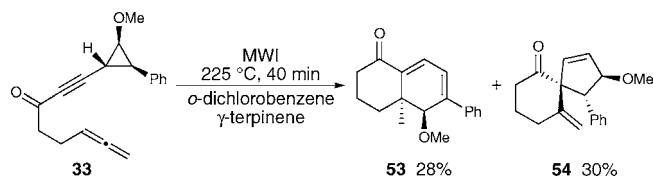
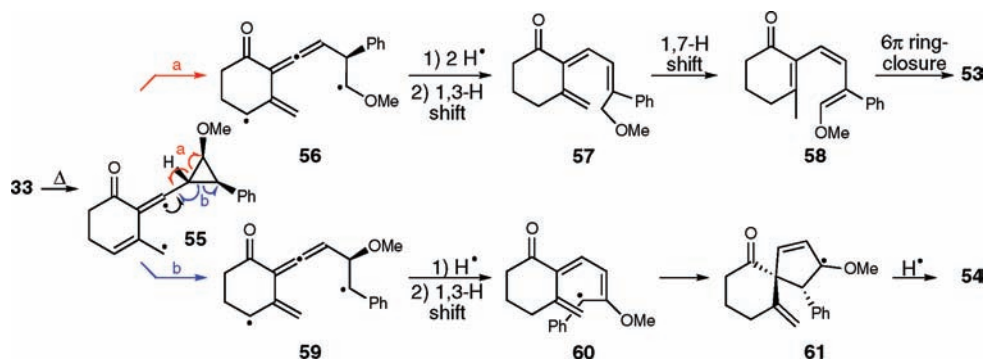


Figure 14. Microwave irradiation of allene-ynone **33**. The stereochemistry of **53** and **54** was not assigned experimentally, but was assigned by comparison of the experimental spectra to the spectra predicted by Spartan '08 (see Supporting Information).

structure is exergonic. This is likely due to several factors, including trading a σ -bond for a π -bond, as well as the creation of a more planar π -system, which allows for more delocalization. All of this information suggests that the mechanism in Scheme 3 is plausible.

In one further attempt to detect reactive intermediates along the cycloaddition pathway, allene-ynone **33** was heated under microwave conditions (225 °C, 40 min), which led to the formation of two new products **53** and **54** (Figure 14).

Bicyclic diene **53** is reasoned to arise via the mechanism proposed in Scheme 4. Upon heating, bond formation occurs

Scheme 4. Proposed Mechanism for the Formation of **53** and **54**

to give diradical **55**. Opening of the cyclopropane can lead to methoxy stabilized radical **56**. Diradical **56**, after addition of two hydrogen atoms, could then undergo a 1,3-H migration (not a concerted sigmatropic reaction) to produce triene **57**. Compound **57** could then undergo a 1,7-H migration providing triene **58**, which upon a thermal 6π -electrocyclization would produce diene **53**.⁴³

Formation of spirocycle **54** is reasoned to arrive via intermediate **55** just as in the formation **53**. An alternative opening of the cyclopropane in **55** provides the phenyl-stabilized radical in **59**. Compound **59** could then rearrange to triene **60**. Radical cyclization of **60** would produce spirocycle **61**, which can abstract a hydrogen atom to give compound **54**.

Cyclopropanes bearing adjacent methoxy and phenyl groups tend to open on the phenyl side when cyclopropylcarbinyl radicals are formed and on the methoxy side when cyclopropylcarbinyl cations are formed,^{35c,38a} making our proposed mechanism for formation of **53** somewhat unusual. To determine whether alternative zwitterionic pathways may be possible for the conversion of **33** to **53** (and/or **54**), the

geometry of **55** was computed (see Supporting Information for geometry) and an electrostatic potential (ESP) map of this structure appears in Figure 15 (along with an ESP map for **24** for comparison). Comparing ESP maps for **55** and **24**, it becomes clear that **55** harbors no more charge buildup than does **24**, perhaps indicating that zwitterionic pathways for converting **33** to **53** and/or **54** are less likely than the diradical pathways proposed above.

Conclusion

The quantum chemical calculations and experiments described herein provide evidence that the thermal [2 + 2] cycloadditions of allene–ynes likely proceed through step-wise diradical pathways involving intermediates with allylic radical substructures (as in Scheme 1, top). Such pathways are favored over the alternative mode of cyclization (Scheme 1, bottom) and over cycloaddition onto the proximal π -bond of the allene. We continue to investigate this interesting reaction both experimentally and theoretically with an eye

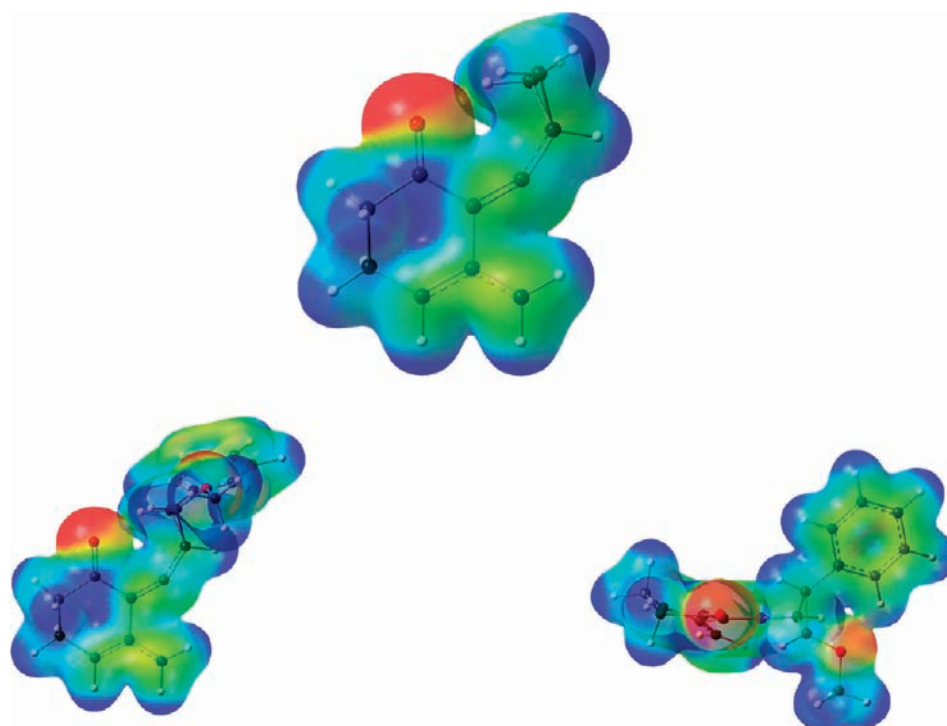


Figure 15. Electrostatic potential (ESP) maps (isoval = 0.01, charge range = $[-4e - 2]$ to $[6e - 2]$) for **24** (top) and two views of **55** (bottom).

toward the design of new systems that react in unusual but predictable ways.

Acknowledgment. D.J.T. and M.R.S. gratefully acknowledge UC Davis and the National Science Foundation's CAREER (CHE-0449845) and Partnership for Advanced Computational Infrastructure (CHE-030089; PSC) programs for support and the ACS Division of Organic Chemistry and Organic Syntheses for their

(43) For examples of thermal allene isomerizations see the following and references therein: Hayashi, R.; Feltenberger, J. B.; Hsung, R. P. *Org. Lett.* **2010**, *12*, 1152–1155.

Graduate Fellowship to M.R.S. K.M.B and J.M.O thank the National Science Foundation for supporting this work (CHE0910597) and Professor Dennis Curran for helpful discussions.

Supporting Information Available: Additional computational details and data, including coordinates, energies, IRC information, and complete ref 21. Experimental procedures as well as NMR spectra and characterizations. This material is available free of charge via the Internet at <http://pubs.acs.org>.

JA102848Z